Two-Dimensional Conduction and CFD Simulations of Heat Transfer in Horizontal Window Frame Cavities

Arild Gustavsen, PhD
Member ASHRAE

Christian Kohler

Dariush Arasteh, PE
Member ASHRAE

Dragan Curcija, PhD
Member ASHRAE

ABSTRACT

Accurately analyzing heat transfer in window frames and glazings is important for developing and characterizing the performance of highly insulating window products. This paper uses computational fluid dynamics (CFD) modeling to assess the accuracy of the simplified frame cavity conduction/convection models presented in ISO 15099 and used in software for rating and labeling window products. Three representative complex cavity cross-section profiles with varying dimensions and aspect ratios are examined. The results presented support the ISO 15099 rule that complex cavities with small throats should be subdivided; however, our data suggest that cavities with throats smaller than 7 mm should be subdivided, in contrast to the ISO 15099 rule, which places the break point at 5 mm. The agreement between CFD modeling results and the results of the simplified models is moderate for the heat transfer rates through the cavities. The differences may be a result of the underlying ISO 15099 Nusselt number correlations being based on studies where cavity height/length aspect ratios were smaller than 0.5 and greater than 5 (with linear interpolation assumed in between). The results presented here are for horizontal frame members because convection in vertical jambs involves very different aspect ratios that require three-dimensional CFD simulations.

INTRODUCTION

The frame is an important part of a fenestration product. In a window with a total area of 1.2×1.2 m^2 and a frame with a width of 10 cm, the frame occupies 30% of the window's total area. If the total area of the window is increased to 2.0×2.0 m^2 and the window still has a frame with a width of 10 cm, the frame occupies 19% of the total area. When rating a fenestration product, engineers area-weight the thermal performance of the different parts of the product to determine a single number that describes the entire product. Thus, to be able to accurately calculate a product's thermal performance, engineers need models that accurately describe the thermal performance of each part of the product or accurate measurements of actual thermal performance. Because measurement is expensive, use of accurate models is preferable.

A significant body of research has focused on heat-transfer effects in glazing cavities. The primary goal of that work has been to develop accurate correlations for natural convection effects inside multiple-pane windows (Batchelor 1954; Eckert and Carlson 1961; Hollands et al. 1976; Raithby et al. 1977; Berkovsky and Polevikov 1977; Korpela et al. 1982; ElSherbiny et al. 1982; Shewen et al. 1996; Wright 1996; Zhao 1998). Less research has been conducted on heat transfer in window frames that have internal cavities. This is an important issue for high-performance window frames because cavities are a primary area where frame heat transfer can be minimized (the thermal conductivity of solid framing materials is another key area). In window frames with internal cavities, the heat-transfer process involves a combination of conduction, convection, and radiation. To fully describe heat transfer through these window frames, it would be necessary to simulate fluid flow to determine the convection effects and to use either view factors or ray-tracing techniques to determine the radiation effects inside the cavities. However, these types of simulations and techniques are rarely undertaken because they require significant computational resources and modeling efforts. Instead, air cavities in window frames are treated as solid materials that have an effective conductivity (Standaert 1984; Jonsson 1985; Carpenter and McGowan

A. Gustavsen is associate professor in the Department of Civil and Transport Engineering, Norwegian University of Science and Technology. **C. Kohler** is computer systems engineer and **D. Arasteh** is staff scientist and deputy group leader, Windows and Daylighting Group, Lawrence Berkeley National Laboratory, Berkeley, California. **D. Curcija** is president of Carli, Inc., Amherst, Mass.

1989); that is, convection and radiation effects are combined into a single effective conductivity. With this single value, standard conduction simulation software can find the insulation value or thermal transmittance (U-factor) of the frame using the same procedure as is used for window frames without internal cavities. The proposed standard ASHRAE 142P and standards EN ISO 10077-2 and ISO 15099 (ASHRAE 1996; CEN 2003; ISO 2003) prescribe methods of this type for finding the thermal transmittance of window frames.

To represent the airflow in frame cavities, various sources prescribe rules for subdividing cavities at points where their dimensions are smaller than a specified minimum. NFRC (Mitchell et al. 2003) and ISO 15099 (ISO 2003) indicate that cavities are to be divided at points where their dimensions are less than 5 mm, and EN ISO 10077-2 (CEN 2003) specifies that cavities with one dimension not exceeding 2 mm or subareas of cavities with interconnection whose size does not exceed 2 mm should be divided into separate subcavities (here, the terms *subarea* and *subcavity* are used for parts of a larger cavity that can naturally be separated from the larger cavity based on its geometric configuration). No research basis is given for the values used in these rules. The standards also differ in their rules for converting nonrectangular (or irregular) cavities into equivalent rectangular cavities whose convection and radiation correlations are assumed to be the same as the correlations for the original irregular cavity. ISO 15099 and EN ISO 10077-2 specify that irregular cavities should be transformed into rectangular cavities so that the areas and aspect ratios of the original irregular cavity and the new rectangular cavity are equal. The proposed ASHRAE Standard 142P specifies that irregular cavities should be transformed into rectangular cavities using a bounding rectangle. The aspect ratios and the total heights and widths of the original irregular cavity and the new rectangular cavity should be equal. (The total heights and widths will most likely not be equal under ISO 15099/EN ISO 10077-2 and ASHRAE 142P.) It is noted that the conversion of irregular cavities to rectangular cavities only is performed for finding the effective conductivity of the irregular cavity. The true geometry is retained for the numerical simulation.

In this paper, focus is put on convective heat transfer in frame cavities; problems related to dividing cavities and transforming irregular cavities into rectangular cavities are addressed. (Radiant heat-transfer effects are not studied.) The results presented are for horizontal frame members because convection in vertical jambs involves very different aspect ratios that require three-dimensional computational fluid dynamics (CFD) simulations. CFD and conduction simulations were conducted for this study. In the conduction simulations, an effective conductivity (calculated according to procedures described in ISO 15099, see below) was used to account for convection in frame cavities.

GEOMETRIES STUDIED

The air cavities studied are shown in Figure 1. The particular cavities were chosen to represent air cavities that can be found in real window frames. The cavities are identified as H-cavity, L-cavity, and C-cavity (left to right in Figure 1). H-cavity is square with two solid fins protruding into it. Dimensions and temperature differences simulated for the cavities are shown in Tables 1 to 3. Because the cavities are simulated in two dimensions, the results are valid for horizontal frame members. CFD results that are valid for jamb sections require simulations in three dimensions.

NUMERICAL PROCEDURE

The simulations were performed with a CFD code (Fluent 1998) and a building component thermal simulation program for implementing ISO 15099 (Finlayson et al. 1998). Double precision was used for both codes.

CFD Simulations

The CFD code uses a control-volume method to solve the coupled heat and fluid flow equations. Only conduction and natural convection are simulated; radiation effects are not addressed. The maximum Rayleigh number found for the cavities studied is about 1×10^5. This Rayleigh number is found for the H-cavity when there is a temperature difference of 25 K separating the two isothermal walls. Ostrach (1988)

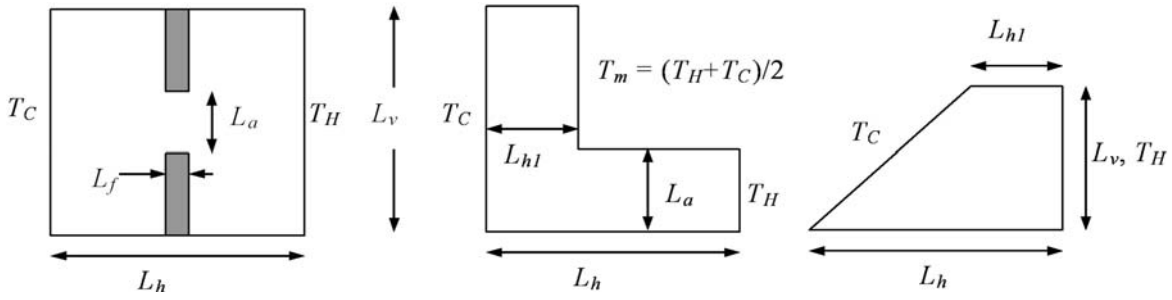

Figure 1 *Schematics of cavities studied. From left to right—H-cavity, L-cavity, and the C-cavity.*

Table 1. Cavity Dimensions and Temperatures for the H-Cavity

ID	L_v [mm]	L_h [mm]	L_a [mm]	L_f [mm]	T_H [°C]	T_C [°C]
H1	30	30	30	-	15	-10
H2	30	30	20	2	15	-10
H3	30	30	15	2	15	-10
H4	30	30	10	2	15	-10
H5	30	30	7	2	15	-10
H6	30	30	5	2	15	-10
H7	30	30	3	2	15	-10
H8	30	30	0	2	15	-10
H9	30	30	30	-	15	5
H10	30	30	20	2	15	5
H11	30	30	15	2	15	5
H12	30	30	10	2	15	5
H13	30	30	7	2	15	5
H14	30	30	5	2	15	5
H15	30	30	3	2	15	5
H16	30	30	0	2	15	5

Table 2. Cavity Dimensions and Temperatures for the L-Cavity

ID	L_v [mm]	L_h [mm]	L_{h1} [mm]	L_a [mm]	T_H [°C]	T_C [°C]
L1	30	30	10	15	15	-10
L2	30	30	10	10	15	-10
L3	30	30	10	7	15	-10
L4	30	30	10	5	15	-10
L5	30	30	10	3	15	-10
L6	30	30	10	15	15	5
L7	30	30	10	10	15	5
L8	30	30	10	7	15	5
L9	30	30	10	5	15	5
L10	30	30	10	3	15	5

Table 3. Cavity Dimensions and Temperatures for the C-Cavity

ID	L_v [mm]	L_h [mm]	L_{h1} [mm]	T_H [°C]	T_C [°C]
C1	20	30	10	15	-10
C2	20	30	10	15	5
C3	10	30	10	15	-10
C4	10	30	10	15	5

reports steady laminar flow for square cavities of this size. Although most of the cavities presented are not squares, incompressible and steady laminar flow are assumed. Further, viscous dissipation is not addressed, and all thermophysical properties are assumed to be constant except for the buoyancy term of the y-momentum equation where the Boussinesq approximation is used. The Semi-Implicit Methodf or Pressure-linked Equations Consistent (SIMPLEC) was used to model the interaction between pressure and velocity. The energy and momentum variables at cell faces were found by using the Quadratic Upstream Interpolation for Convective Kinetics (QUICK) scheme. In addition, the CFD code uses central differences to approximate diffusion terms and relies on the PREssure Staggering Option scheme (PRESTO) to find the pressure values at the cell faces. PRESTO is similar to the staggered grid approach described by Patankar (1980). Convergence is determined by checking the scaled residuals and ensuring that they are less than 10^{-5} for all variables, except for the energy equation, in which the residuals have to be less than 10^{-6}.

A quadrilateral grid was used for all cavities. Some grid sensitivity tests were performed for the H- and C-cavities. The L-cavity was assumed to behave similarly to the H-cavity with respect to grid density; therefore, the same grid density was used for the L-cavity as for the H-cavity. For the H-cavity, the grid size was varied between 0.5 mm and 0.06 mm, where the first size results in 3,600 nodes and the latter size results in 249,999 nodes. For the C-cavity, grid sizes of 0.5 mm, 0.1 mm, and 0.05 mm were tested, resulting in 2,369, 28,919, and 227,195 nodes, respectively. An interval size of 0.1 mm was found to be sufficient for all cavities. Reducing the grid sizes to 0.06 mm for the H-cavity and 0.05 mm for the C-cavity resulted in changes of heat fluxes of less than 0.5%.

Conduction Simulations

The conduction simulations were performed using a special version of the building component thermal simulation program in which the radiation calculation in frame cavities was disabled, which allowed a comparison of the convection effects with the CFD calculations. A finite-element approach was used to solve the conductive heat transfer equation. The quadrilateral mesh is automatically generated. Refinement was performed in accordance with section 6.3.2b. of ISO 15099 (ISO 2003). The energy error norm was less than 10% in all cases, which results in an error of less than 1% in the thermal transmittance of the cavities. The temperatures on the boundaries of the cavities were fixed using a very large combined convective and radiative film coefficient (h = 99,900 W m^{-2} K^{-1}). The resulting cavity wall temperatures were within 0.01°C of the desired temperatures. For more information on the thermal simulation program algorithms, refer to Appendix C in Finlayson et al. (1998).

The procedures and the natural convection correlations used to find the effective conductivities of the cavities according to ISO 15099 are listed below. Note that only correlations for horizontal frame members are used in this study. The effective conductivity is determined from

$$\lambda_{eff} = (h_{cv} + h_r) \times L \,, \tag{1}$$

where λ_{eff} is the effective conductivity, h_{cv} is the convective heat transfer coefficient, h_r is the radiative heat transfer coefficient (set equal to zero in this study), and L is the thickness or width of the air cavity in the direction of heat flow. The convective heat transfer coefficient, h_{cv}, is calculated from the Nusselt number (Nu) from

$$h_{cv} = \mathrm{Nu}\frac{\lambda_{air}}{L} \,, \tag{2}$$

where λ_{air} is the conductivity of air.

For horizontal heat flow, the Nusselt number will depend on the height-to-length aspect ratio (L_v/L_h), where L_v and L_h are the cavity dimensions in the vertical and horizontal directions, respectively. In a cavity with a height-to-length aspect ratio less than 0.5, the Nusselt number is found from (Rosenhow et al. 1985),

$$\mathrm{Nu} = 1 + \left\{ \left[2.756 \times 10^{-6} \mathrm{Ra}^2 \left(\frac{L_v}{L_h} \right)^8 \right]^{-0.386} + \left[0.623 \mathrm{Ra}^{1/5} \left(\frac{L_h}{L_v} \right)^{2/5} \right]^{-0.386} \right\}^{-2.59} \,, \tag{3}$$

where Ra is the Rayleigh number and is defined as

$$\mathrm{Ra} = \frac{\rho_{air}^2 L_h^3 g \beta c_{p,air} (T_H - T_C)}{\mu_{air} \lambda_{air}} \,, \tag{4}$$

where ρ_{air} is the density of air, g is the acceleration due to gravity, β is the thermal expansion coefficient, and $c_{p,air}$ is the specific heat capacity at constant pressure for air. λ_{air} is the thermal conductivity and μ_{air} is the dynamic viscosity of air. $T_H - T_C$ is the temperature difference between the warm and the cold walls of the rectangular cavity. For a cavity with a height-to-length aspect ratio (L_v/L_h) larger than 5, the Nusselt number is found from (Wright 1996),

$$\mathrm{Nu} = max(\mathrm{Nu}_1, \mathrm{Nu}_2, \mathrm{Nu}_3) \,, \tag{5}$$

where

$$\mathrm{Nu}_1 = \left\{ 1 + \left(\frac{0.104 \mathrm{Ra}^{0.293}}{\left[1 + \left(\frac{6310}{\mathrm{Ra}} \right)^{1.36} \right]} \right)^3 \right\}^{1/3} \tag{6}$$

$$\mathrm{Nu}_2 = 0.242 \left(\mathrm{Ra} \frac{L_h}{L_v} \right)^{0.273} \tag{7}$$

$$\mathrm{Nu}_3 = 0.0605 \mathrm{Ra}^{1/3} \tag{8}$$

For cavities with L_v/L_h between 0.5 and 5, the Nusselt number is found using a linear interpolation between the endpoints of Equations 3 and 5.

For heat flow upward, the situation is unstable. The Nusselt number here is also dependent on the height-to-length aspect ratio L_v/L_h of the air cavity. For L_h/L_v less than or equal to 1, the convection is restricted by wall friction and the Nusselt number is equal to 1. For $1 < L_h/L_v \leq 5$, the Nusselt number is calculated according to (Rosenhow et al. 1985):

$$\mathrm{Nu} = 1 + \left(1 - \frac{\mathrm{Ra}_{cr}}{\mathrm{Ra}}\right)^{\bullet} [k1 + 2(k2)^{1-\ln k2}] + \left[\left(\frac{\mathrm{Ra}}{5830}\right)^{1/3} - 1\right]^{\bullet} \left[1 - e^{-0.95\left(\left(\frac{\mathrm{Ra}_{cr}}{\mathrm{Ra}}\right)^{1/3} - 1\right)^{\bullet}}\right] \quad (9)$$

where

$$k1 = 1.40 \quad (10)$$

$$k2 = \frac{\mathrm{Ra}^{1/3}}{450.5} \quad (11)$$

$$(X)^{\bullet} = \frac{X + |X|}{2} \quad (12)$$

$$\mathrm{Ra}_{cr} = e^{\left(0.721\frac{L_v}{L_h}\right) + 7.46} \quad (13)$$

For L_h/L_v larger than 5, the Nusselt number is (Hollands et al. 1976)

$$\mathrm{Nu} = 1 + 1.44\left(1 - \frac{1708}{\mathrm{Ra}}\right)^{\bullet} + \left[\left(\frac{\mathrm{Ra}}{5830}\right)^{1/3} - 1\right]^{\bullet}. \quad (14)$$

The Rayleigh number (Ra) in Equations 9 and 14 can be calculated from Equation 4 but with L_h replaced by L_v.

For heat flow downward, the Nusselt number is equal to 1.0.

For jamb frame sections, frame cavities are oriented vertically, and therefore the height of the cavity is in the direction normal to the plane of the cross section. For these cavities, it is assumed that heat flow is always in horizontal direction with $L_v/L_h > 5$, and so correlations in Equations 6 to 8 shall be used.

The temperatures of the cavity walls, T_H and T_C, are not known in advance, so it is necessary to estimate them. From previous experience it is recommended to apply T_H = 10°C and T_C = 0°C. However, after the simulation is done, it is necessary to update these temperatures from the results of the previous run. This procedure shall be repeated until values of T_H and T_C from two consecutive runs are within 1°C. Also, it is important to inspect the direction of heat flow after the initial run because if the direction of the bulk of heat flow is different than initially specified, it will need to be corrected for the next run.

According to ISO 15099 (ISO 2003), unventilated and irregular (not rectangular) frame cavities are converted into equivalent rectangular cavities. The transformation is conducted so that the areas and aspect ratios of the original irregular cavity and the new rectangular cavity are equal. Further, if the shortest distance between two opposite surfaces is smaller than 5 mm, then the frame cavity is split at this throat region. The following rules are used to determine which surfaces belong to vertical and horizontal surfaces of the equivalent rectangular cavity (0° is east [right], 90° is north [up], 180° is west [left], and 270° is south [bottom]):

- any surface whose normal is between 315° and 45° is a left vertical surface;
- any surface whose normal is between 45° and 135° is a bottom horizontal surface;
- any surface whose normal is between 135° and 225° is a right vertical surface;
- any surface whose normal is between 225° and 315° is a top horizontal surface.

Temperatures of equivalent vertical and horizontal surfaces are calculated as the mean of the surface temperatures according to the classification above. The direction of heat flow is determined from the temperature difference between vertical and horizontal surfaces of the equivalent rectangular cavity. The following rules are used:

- Heat flow is horizontal if the absolute value of the temperature difference between vertical cavity surfaces is larger than between horizontal cavity surfaces.
- Heat flow is vertical and upward if the absolute temperature difference between horizontal cavity surfaces is larger than between vertical cavity surfaces and the temperature difference between the top horizontal cavity surface and bottom horizontal cavity surface is negative.
- Heat flow is vertical and downward if the absolute temperature difference between horizontal cavity surfaces is larger than between vertical cavity surfaces and the temperature difference between the top horizontal cavity surface and bottom horizontal cavity surface is positive.

Illustrations and more information can be found in ISO 15099.

Boundary Conditions and Material Properties

The air properties used in the CFD simulations are calculated at mean temperature, $(T_H+T_C)/2$, and atmospheric pressure, P = 101325 Pa, and are shown in Table 4. The standard acceleration of gravity of 9.8 m/s^2 was used in all calculations. Constant temperature boundary conditions are specified at all vertical walls and at the sloped wall of the C-cavity (see Figure 1). All horizontal walls are adiabatic. The conductivity of the fin in the H-cavity is set to 0.25 W m^{-1} K^{-1}.

RESULTS

Heat Transfer Rates for the H-cavity and the L-cavity—CFD Results

Heat fluxes for different gap openings, L_a, are plotted for the H-cavity and L-cavity. For the H-cavity, the heat flux is found from

Table 4. Air Properties Used in the CFD Simulations

$(T_H+T_C)/2$ [°C]	λ [W m^{-1} K^{-1}]	c_p [J kg^{-1} K^{-1}]	μ [kg m^{-1} s^{-1}]	ρ [kg m^{-3}]	β [K^{-1}]
2.5	0.024253	1005.2	1.7357×10^{-5}	1.2807	$3{,}6278 \times 10^{-3}$
10	0.024817	1005.5	1.7724×10^{-5}	1.2467	$3{,}5317 \times 10^{-3}$

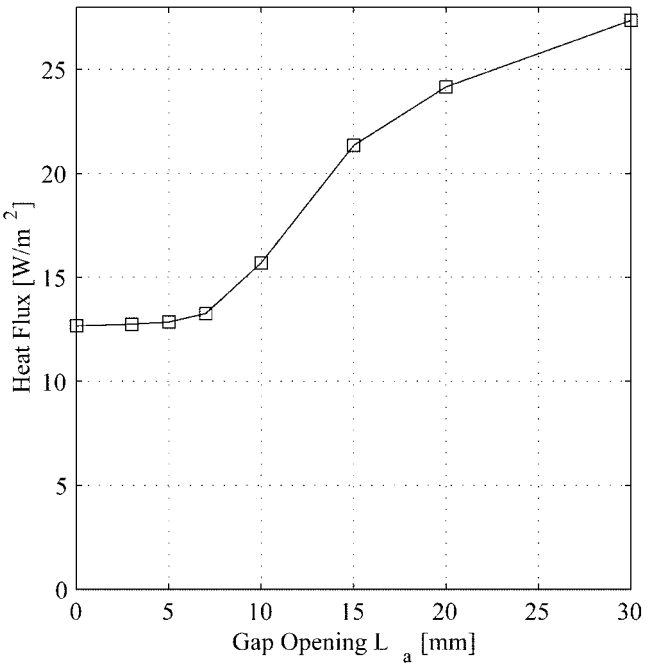

Figure 2 *Graph of heat flux from the CFD simulation through warm side of the H-cavity as function of gap opening, L_a. The temperature difference between warm and cold surfaces is 10°C.*

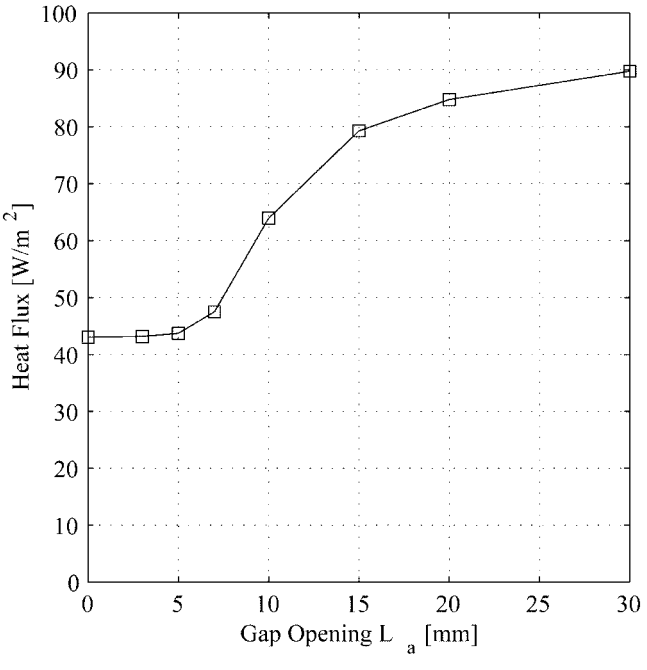

Figure 3 *Graph of heat flux from the CFD simulation through warm side of the H-cavity as function of gap opening, L_a. The temperature difference between warm and cold walls is 25°C.*

$$q = Q / L_v, \tag{15}$$

where Q is the heat flow through the warm side of the cavity and L_v is the height of the cavity (equal to 30 mm for all H-cavities). For the L-cavity, the heat fluxes are calculated according to:

$$q_{Total} = (Q_{TH} + Q_{Tm})/L_v \tag{16}$$

$$q_{TH} = Q_{TH}/L_a \tag{17}$$

$$q_{Tm} = Q_{Tm}/L_{Tm} \tag{18}$$

where Q_{TH} and Q_{Tm} are the heat flows through the parts of the cavity having temperatures T_H and T_m, respectively, and L_a and L_{Tm} are the lengths of the respective parts of the cavity. L_{Tm} is equal to the height of the cavity (L_v) minus L_a.

Figure 2 and Figure 3 show the heat flux from the CFD calculations through the warm wall of the H-cavity as a function of gap opening, L_a, for temperature differences between the warm and cold walls of 10°C and 25°C, respectively. The vertical axis shows the heat flux in W/m^2, and the horizontal axis shows the gap opening in millimeters.

Figure 4 and Figure 5 show the heat fluxes from the CFD simulation through the cavity walls with temperatures T_H and T_m and the total fluxes for the L-cavity as function of gap opening for temperature differences between the warm and cold surfaces of 10°C and 25°C, respectively. The vertical axis shows the heat flux in W/m^2, and the horizontal axis shows the gap opening, L_a, in millimeters.

Stream Contours

Insight into the airflow in frame cavities may also be gained by looking at the stream contours for the different cavities. Figure 6 displays stream contours for the H-cavity. The diagrams in the left column display results for the cases in which the temperature difference between the warm and cold

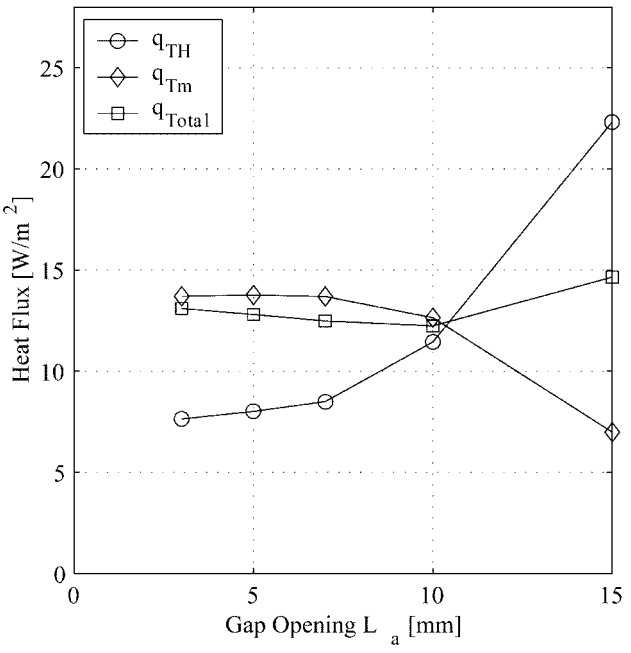

Figure 4 *Graph of the heat fluxes from the CFD simulation through the cavity walls with temperatures T_H and T_m and the sum of the fluxes for the L-cavity as function of gap opening, L_a. The temperature difference between warm and cold surfaces is 10°C.*

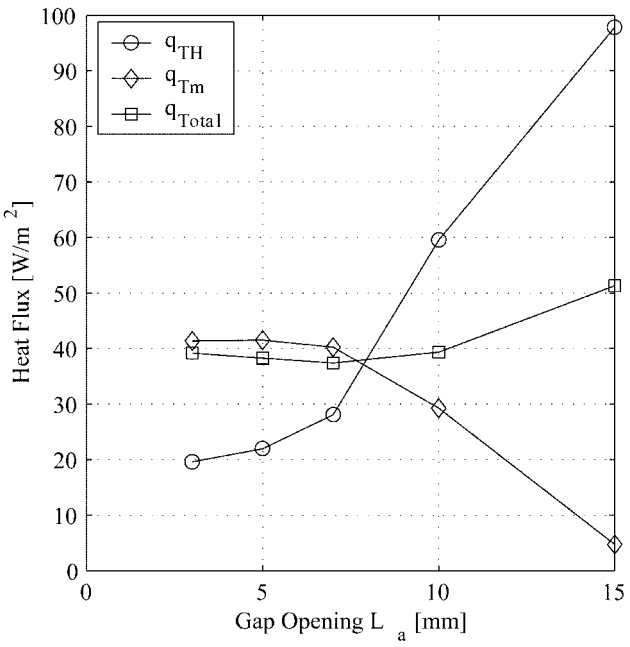

Figure 5 *Graph of the heat fluxes from the CFD simulation through the cavity walls with temperatures T_H and T_m and the sum of the same fluxes for the L-cavity as function of gap opening, L_a. The temperature difference between warm and cold surfaces is 25°C.*

walls is 10°C, and the right diagrams show results where the temperature difference is 25°C. Each row includes results for different gap openings, L_a (see the geometry to the left in Figure 1). The magnitude of the stream contours is set automatically by the CFD program, and the contour lines are distributed at even intervals between the maximum and minimum values for each case.

Figure 7 displays stream contours for the various versions of the L-cavity. The left column diagrams show results for the cases where the temperature difference between the warm and cold walls is 10°C, and the right diagrams show results where the temperature difference is 25°C. Each row includes results for different gap openings, L_a.

Figure 8 shows the stream contours for the versions of the C-cavity. The left and right columns display results where the temperature differences are 10°C and 25°C, respectively. Each row corresponds to a fixed cavity height, L_v. The various diagrams show that there is little circulation close to the corners with sharp angles. By making tangents to the outer stream contour line for each cavity (close to the sharp corners), we find the measures 6.6, 6.3, 8.8, and 7.5 mm for the lengths of the tangents (from left to right, line by line).

Comparison of CFD and ISO 15099 Convection Correlations

Although there are several correlations and procedures for finding effective conductivity, we focused on those presented in ISO 15099. To check the accuracy of these correlations and procedures, the CFD results are compared with conduction simulations based on ISO 15099. Results for the H-cavity are shown in Figures 9 and 10 for the cases where the temperature differences between the warm and cold surfaces are 10°C and 25°C, respectively. Results for the L-cavity are shown in Figures 11 and 12 for the cases where the temperature differences between the warm and cold surfaces are 10°C and 25°C, respectively. The vertical axis shows the heat flux in W/m^2, and the horizontal axis shows the gap opening, L_a, in millimeters. The graphs are labeled as follows:

- "CFD" signifies the results from the CFD simulation.
- "ISO 15099" denotes the heat fluxes that were calculated in the building component thermal simulation program according to ISO 15099; for these examples, the air cavity was divided when the distance between two opposite surfaces was smaller than 5 mm. Thus, for the H-cavity, the air cavity was divided when the interconnection formed by the fins was smaller than 5 mm, resulting in three separate air cavities. (If the distance

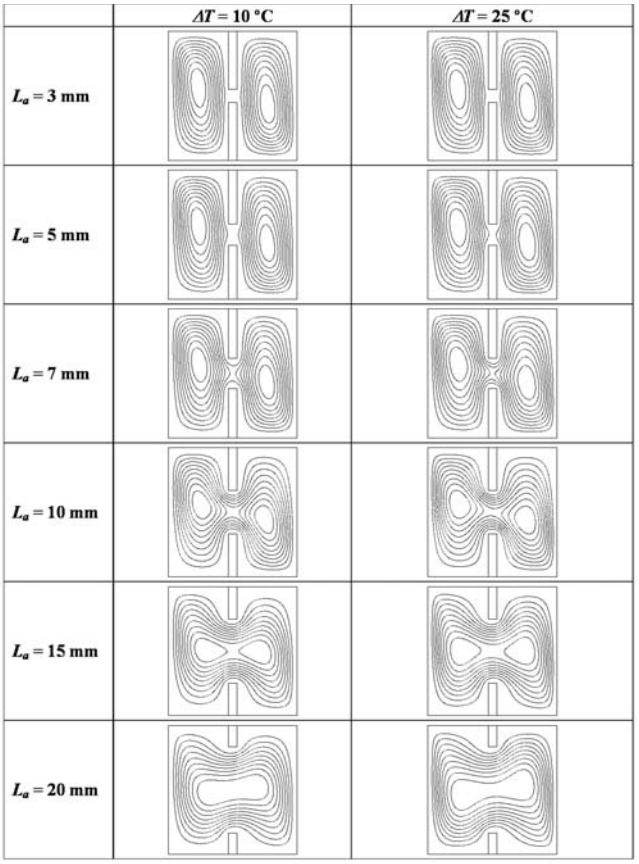

Figure 6 *Stream contours for the H-cavities. L_a is the size of the gap opening, and T is the difference between the hot and cold wall temperatures, reported in °C.*

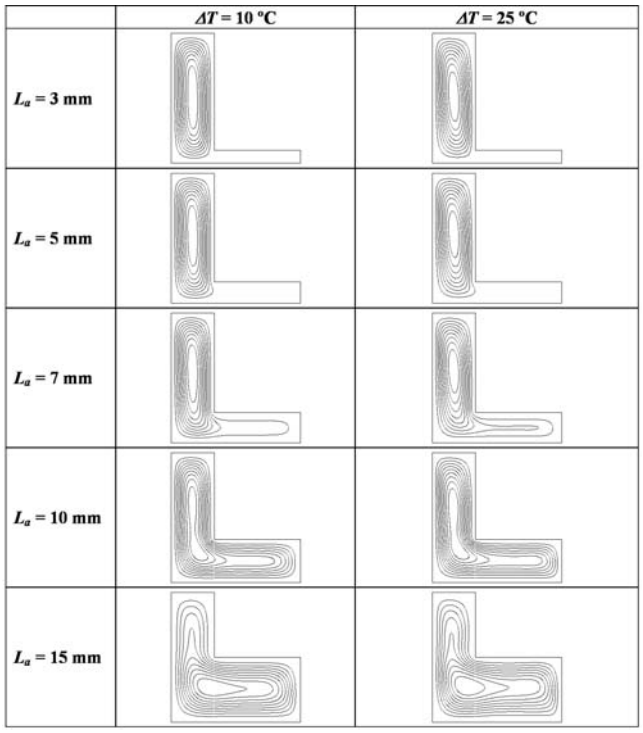

Figure 7 *Stream contours for the L-cavities. L_a is the size of the gap opening, and T is the difference between the hot and cold wall temperatures, reported in °C.*

between the fins in the air cavity was equal to 5 mm or more there was no division.)

Table 5 shows heat fluxes for the C-cavity as a function of temperature difference and air cavity height. The table includes, in addition to CFD results, results from conduction simulations where an effective conductivity was used to account for convection. These were carried out both with a 5-mm vertical division of the air cavity in the sharp angle of the cavity (column labeled "5-mm Rule") and no division of the air cavity (column labeled "No Division"). Results are included for temperature differences between the warm and cold walls equal to 10°C and 25°C.

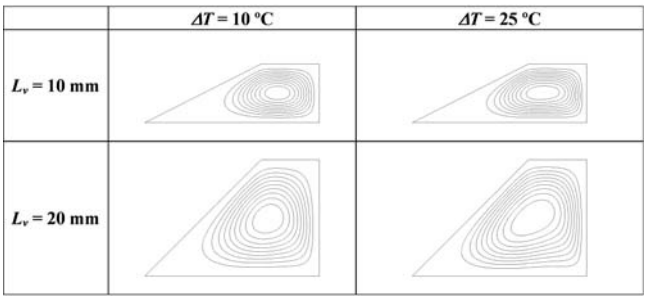

Figure 8 *Stream contours for the C-cavities for different temperature differences, ΔT. L_v is the height of the cavity.*

DISCUSSION

As noted in the introduction to this paper, various rules address the break point at which to divide air cavities in window frames. In this section, the results from the previous section are analyzed in detail to determine the point at which frame air cavities should be divided. A discussion of the agreement between the CFD results and the procedures in ISO 15099 for calculating heat flow through air cavities of window frames is also included.

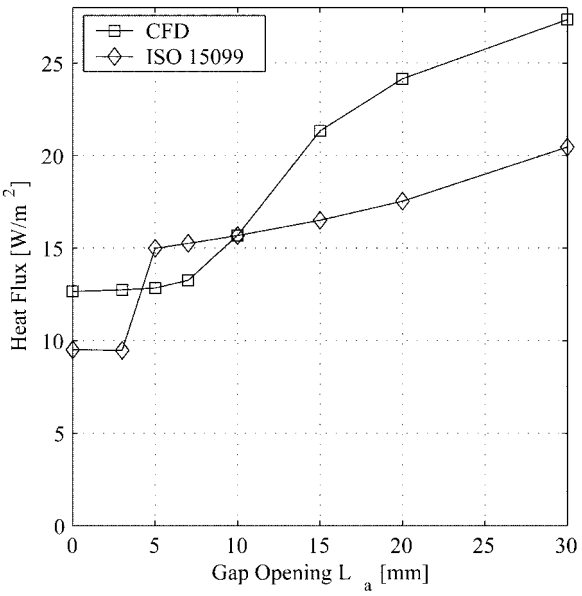

Figure 9 *Comparison of heat fluxes from CFD and conduction simulations for the H-cavity as a function of gap opening L_a. The temperature difference between the warm and the cold surfaces is 10°C.*

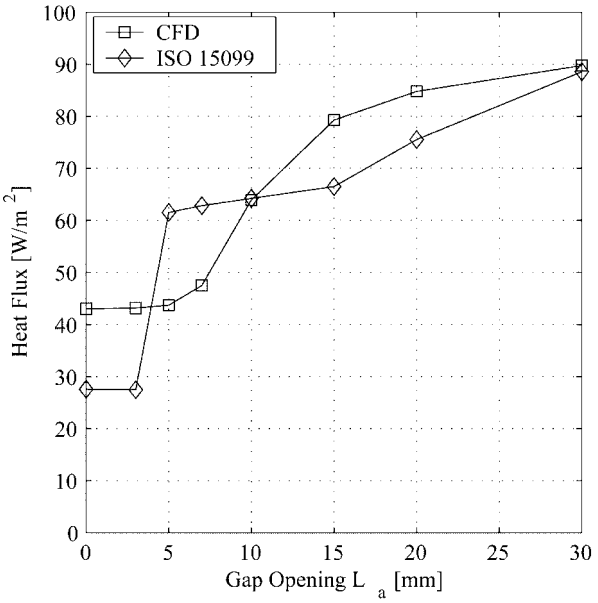

Figure 10 *Comparison of heat fluxes from CFD and conduction simulations for the H-cavity as a function of gap opening L_a. The temperature difference between the warm and the cold surfaces is 25°C.*

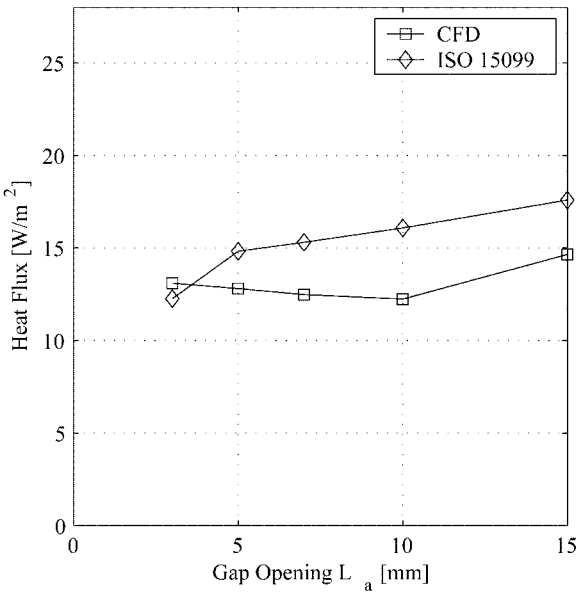

Figure 11 *Comparison of heat fluxes from CFD and conduction simulations for the L-cavity as a function of gap opening L_a. The temperature difference between the warm and the cold surfaces is 10°C.*

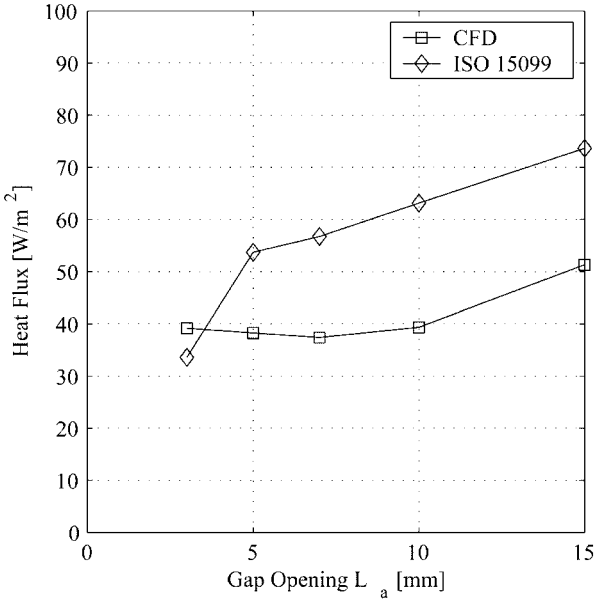

Figure 12 *Comparison of heat fluxes from CFD and conduction simulations for the L-cavity as a function of gap opening L_a. The temperature difference between the warm and the cold surfaces is 25°C.*

Table 5. Comparisons of Heat Fluxes for the C-Cavity

	Heat Flux [W/m^2]					
	ΔT = 10°C			ΔT = 25°C		
L_v [mm]	CFD	No Division	5-mm Rule	CFD	No Division	5-mm Rule
10	23.65518	19.996	23.063	87.3778	63.9525	87.4525
20	31.57198	28.272	20.195	105.04675	123.675	71.7

Heat Transfer Rates and Contour Plots—Cavity Division Rule

Heat-transfer rates and stream contour plots were reported above for all cavities. Figures 2 and 3 display the heat fluxes for the H-cavity as a function of gap opening for T equal to 10°C and 25°C, respectively. In both cases, the heat flow is fairly constant for gap openings less than 5 to 7 mm. When the gap opening increases from 7 to 10 mm, the increase in heat flux is more pronounced. These results suggest that air cavities should be divided when the gap opening is less than 7 mm. However, when the temperature difference between the warm and cold walls increases, the heat flux increases for smaller gap openings. For the L-cavity, the total heat flux is fairly constant for all gap openings. At the same time, the part fluxes through the surfaces having temperatures of T_{H} and T_{m} change more when the gap opening is larger than 5 to 7 mm.

The stream contour diagrams for the H-cavity (Figure 6) show that the airflow is partly separated between the two subcavities, primarily for gap openings smaller than or equal to 5 mm. For a gap opening equal to 7 mm, there is more airflow between the two subcavities. The graphs show that the air exchange between the subcavities increases when the gap opening is larger than 7 mm. Similar observations may be made for the L-cavity (Figure 7). Little airflow occurs in the small subcavity compared to the airflow in the higher part of the cavity, as long as the height of the subcavity, L_a, is less than or equal to 5 mm. When the height of the subcavity increases to 7 mm and larger, air circulation is more pronounced throughout the entire cavity.

For the C-cavity (Figure 8), the contour plots show that there is limited air circulation in the sharp corner of the cavity.

Based on the CFD simulations, it seems that a 5 to 7 mm rule should be applied when dividing air cavities in window frames.

Comparison of CFD and ISO 15099 Convection Correlations

Figures 9 to 12 and Table 5 show a comparison between the heat transfer rates of the CFD and ISO 15099 calculations. Although a few numbers are comparable, most are not. Nonetheless, for the H-cavity in Figures 9 and 10, the shape of the curves is somewhat similar. The graphs for the L-cavity differ more strongly. The maximum deviations between the CFD and ISO 15099 results are 27% and 41% for the H-cavity with T equal to 10°C and 25°C, respectively. For the L-cavity the comparable results are 31% and 60%.

It is important to note that for the H-cavity, there are two reasons for the reduction of heat flux as the gap opening decreases from 30 mm to 5 mm. One is that the increased fin size prevents air from advecting energy directly across the cavity from one wall to the other; the other is the decrease in effective temperature difference across the cavity, even though the temperatures of the hot and cold walls of the original cavity are fixed. The effective temperature difference decreases because, according to ISO 15099, the temperature of each wall in the original irregular cavity is assigned to a wall in the new rectangular cavity depending on the orientation of the normal vector of the original wall (see ISO 15099 calculation procedures above). Thus, the irregular cavity's vertical fin surfaces are divided between the hot and cold walls in the new rectangular cavity, and new warm and cold wall temperatures are then calculated. Because the fins are in the middle of the cavity and therefore have a temperature approximately equal to the average of T_H and T_C, the result will be a reduced temperature difference across the cavity. This again reduces the effective conductivity of the enclosure.

Two of the H-cavity configurations studied did not include division of air cavities to calculate heat flux. These are the H-cavity with no fins protruding into the cavity (L_a = 30 mm in Figures 9 and 10) and the H-cavity with one fin separating two air enclosures (L_a = 0 in Figures 9 and 10). The former results in a simple square cavity while the latter results in two cavities with height-to-length aspect ratio of 30/14 (2.14) separated by two-mm-thick solid fin. For these cavities, no large differences would be expected between the CFD and the ISO 15099 correlations. Also, the square air cavity results do not differ significantly for the T = 25°C case, but they do differ significantly for the T = 10 °C case. There are also large differences between the CFD and the ISO 15099 results for the configuration where one fin separates two enclosures (both for T = 10°C and 25°C). The reason for these differences is the lack of accuracy of the horizontal heat-flow natural convection correlations between L_v/L_h = 0.5 and L_v/L_h = 5, in which the equivalent conductivity is found by interpolation. The good agreement for the no-fin configuration where T = 25°C is mainly a result of chance. The lack of accuracy for the ISO 15099 convection correlation has been noted by Gustavsen (2001). If the natural convection correlations for frame cavities were more accurate, greater agreement in results would be expected. In addition to above modeled cavities, we conducted

an extra study to evaluate the accuracy of the convection correlation in ISO 15099. A cavity 30 mm high and 14 mm wide containing only air were used. This cavity has the same dimensions as the two air cavities in the 30 by 30 mm cavity with a two-mm-wide fin in the middle. Temperatures of –10°C and 2.5°C were used. The CFD and ISO 15099 simulations resulted in 41.36 and 27.94 W/m^2, respectively. These figures equal Nusselt numbers of 1.95 from the CFD simulation and 1.32 from the ISO 15099 calculations.

The fluxes for the C-cavity are shown in Table 5. For the cavities that have heights (L_v) of 10 mm, the heat flux for the divided cavity is greater than for the undivided cavity. This seems unexpected because dividing frame cavities usually reduces convection, so a division would be assumed to produce a smaller heat flux. However, the increased heat flux after division of the air enclosure in this case may be explained by the change in height-to-length aspect ratio of the cavities from before the division of cavity to after. For the original cavity, the height-to-length aspect ratio is smaller (L_v/L_h = 0.33) than for the largest cavity in the divided case (L_v/L_h = 0.5). For smaller aspect ratios (for cavities with L_v/L_h less than 1), natural convection is suppressed, so lower fluxes are found for the undivided cases. For these cases (L_v = 10 mm), good agreement is also found between CFD and divided cavity results (the ISO 15099 convection correlations for $L_v/L_h < 0.5$ are assumed to be correct because they are based on analytical considerations). For the C-cavities with a height of 20 mm, dividing the cavity reduces the heat flux, but this does not bring the results closer to the CFD results. Here all cavities have aspect ratios within the interpolation range of the ISO 15099 correlation.

The influence of this difference for horizontal frame cavity convective heat transfer (ranging from 27% to 60% as shown in Figures 9, 10, 11, and 12) on the total (horizontal and vertical) frame U-factor and on the overall window U-factor will vary depending on the frame/window construction and overall window size. A change in the horizontal frame cavity convective heat transfer of a given percentage will result at most in a same percentage change (see Equation 1) in the horizontal frame cavity effective conductivity. The maximum percent change would occur when the cavity radiation effects can be neglected, such as those for low-emittance (i.e., reflective) frame cavity surfaces. Since almost all frame cavity surfaces have much higher emittances, the cavity frame radiant heat transfer is of the same order as the frame cavity convective heat transfer. Thus, the percent change in the cavity effective conductivity will be less than the percent change in the cavity convective heat transfer. A simple investigation was performed to estimate the effect that the lack of accuracy in horizontal frame cavity convective heat transfer may have on the total frame and overall window U-factor. This investigation was performed for a vinyl frame with steel reinforcement and an aluminum frame that were used in 1.2 m by 1.2 m windows. The glazing and spacer (edge-of-glass characteristics) configuration was assumed to be constant. An improvement in the accuracy of the horizontal frame cavity convection correlation of 50% may lead to a change in the effective conductivity of the horizontal frame cavities of 25%. This result is valid if the radiation and convection effects are of the same magnitude and if the radiation effects are unchanged. For the particular frames studied, assuming that the horizontal frame lengths were the same as the vertical frame lengths, the change of the total frame U-factors was 7.4% and 5% for the vinyl and aluminum frames, respectively. In the calculations, the horizontal air cavities were replaced by solid material with the 25% change from the ISO 15099 predicted value and the vertical air cavities used the current ISO 15099 predicted values. This results in a change of the overall window U-factors of 2.4% for the vinyl-framed window and 1.8% for the aluminum-framed window. Using the ISO 15099 procedure, the overall U-factor for the vinyl window was calculated to be 1.4 W/m^{2}K. For the aluminum-framed window, the overall U-factor was calculated to be 1.7 W/m^{2}K.

CONCLUSIONS

Based on our results and discussion, the authors conclude that irregularly shaped frame cavities should be divided at points where their dimensions are in the range of 5 to 10 mm; analyzing the heat transfer plots suggests that 7 mm is an appropriate break point. This rule should apply to any constrictions in cavity volume, even in triangular cavities. The heat flux results from CFD and conduction simulations based on ISO 15099 show good agreement in the case of certain cavity configurations. For other aspect ratios, the difference between the two calculation methods is quite significant even for simple rectangular cavities. This difference is a result of the limitation in the linear interpolation that is used in ISO 15099 for frame cavities with an aspect ratio between 0.5 and 5.

The effects of the changes in the horizontal frame cavity heat transfer on the overall U-factors for the windows are small (1.8% to 2.4%) enough to show that the current window horizontal frame cavity calculation procedures in ISO 15099 are sufficiently accurate for different cavity shapes and orientations for obtaining accurate overall window U-factors. If the uncertainty of the overall U-factor—using window hot box methods as in ASTM Standard C1199 and ISO Standard 12567 (ASTM 2000; ISO 2000)—attains levels of 2% to 3% from the current best values of 5% to 6% (Yuan 2002), the inclusion of improved horizontal and vertical frame cavity heat transfer correlations in ISO 15099 might be warranted. Also, if rating and comparison of individual window frames are wanted, the current results suggest that the horizontal frame cavity heat transfer procedures should be improved.

ACKNOWLEDGMENTS

This work was supported by Hydro Aluminum and the Assistant Secretary for Energy Efficiency and Renewable Energy, Office of Building Technology, State and Community Programs, Office of Building Systems of the U.S. Department of Energy under Contract No. DE-AC03-76SF00098. We

would like to thank Nan Wishner, Lawrence Berkeley National Laboratory, for editorial assistance.

REFERENCES

ASHRAE. 1996. Draft BSR/ASHRAE Standard 142P, Standard method for determining and expressing the heat transfer and total optical properties of fenestration products. Atlanta: American Society of Heating, Refrigerating and Air-conditioning Engineers, Inc.

ASTM. 2000. *C1199-00, Standard Test Method for Measuring the Steady-State Thermal Transmittance of Fenestration Systems Using Hot Box Methods*. West Conshohocken, PA: ASTM International.

Batchelor, G.K. 1954. Heat transfer by free convection across a closed cavity between vertical boundaries at different temperatures. *Quarterly Applied Mathematics* 12:209-233.

Berkovsky, B.M., and V.K. Polevikov. 1977. Numerical study of problems on high-intensive free convection. In *Heat Transfer and Turbulent Buoyant Convection* (D.B. Spalding and N. Afgan, eds.), Vol. II, pp. 443-455. Washington: Hemisphere Publishing Corporation.

Carpenter, S.C., and A.G. McGowan. 1989. Frame and spacer effects on window U-value. *ASHRAE Transactions* 95(2):604-608.

CEN. 2003. *EN ISO 10077-2:2003, Thermal performance of windows, doors and shutters—Calculation of thermal transmittance, Part 2: Numerical method for frames*. Brussels: European Committee for Standardization.

Eckert, E.R.G., and W.O. Carlson. 1961. Natural convection in an air layer enclosed between two vertical plates with different temperatures. *International Journal of Heat and Mass Transfer* 2:106-120.

ElSherbiny, S.M., G.D. Raithby, and K.G.T. Hollands. 1982. Heat transfer by natural convection across vertical and inclined air layers. *Journal of Heat Transfer. Transactions of the ASME* 104:96-102.

Finlayson, E., R. Mitchell, D. Arasteh, C. Huizenga, and D. Curcija. 1998. *THERM 2.0: Program description. A PC program for analyzing the two-dimensional heat transfer through building products.* Berkeley: University of California. (Version 5.2.04 of the code was used in the numerical simulations.)

Fluent 1998. *FLUENT 5 User's Guide*. Lebanon, New Hampshire: Fluent Incorporated.

Gustavsen, A. 2001. Heat transfer in window frames with internal cavities. Ph.D. dissertation, Department of Building and Construction Engineering, Norwegian University of Science and Technology, Trondheim, Norway.

Hallé, S., M.A. Bernier, A. Patenaude, and R. Jutras. 1998. The combined effect of air leakage and conductive heat transfer in window frames and its impact on the Canadian energy rating procedure. *ASHRAE Transactions* 104(1):176-184.

Hollands, K.G.T., T.E. Unny, G.D. Raithby, and L. Konicek. 1976. Free convective heat transfer across inclined air layers. *Journal of Heat Transfer. Transactions of the ASME* 98:189-193.

ISO. 2000. *ISO 12567-1:2000, Thermal performance of windows and doors. Determination of thermal transmittance by hot box method. Part 1: Complete windows and doors*. Geneva: International Organization for Standardization.

ISO. 2003. *ISO 15099:2003(E), Thermal performance of windows, doors and shading devices—Detailed calculations*. Geneva: International Organization for Standardization.

Jonsson, B. 1985. Heat transfer through windows. During the hours of darkness with the effect of infiltration ignored. Document D13:1985. Stockholm: Swedish Council for Building Research.

Jonsson, B. 1998. Intercalibration of thermal transmittance measurements of windows by hot box method. Borås, Sweden: SP Swedish National Testing and Research Institute.

Korpela, S.A., Y. Lee, and J.E. Drummond 1982. Heat transfer through a double pane window. *Journal of Heat Transfer. Transactions of the ASME* 104:539-544.

Mitchell, R., C. Kohler, D. Arasteh, C. Huizenga, J. Carmody, and D. Curcija. 2003. *THERM 5/WINDOW 5 NFRC simulation manual.* Berkeley: Lawrence Berkeley National Laboratory.

Ostrach, S. 1988. Natural convection in enclosures. *Journal of Heat Transfer. Transactions of the ASME* 110:1175-1190.

Patankar, S.V. 1980. *Numerical Heat Transfer and Fluid Flow.* Washington: Hemisphere.

Raithby, G.D., K.G.T. Hollands, and T.E. Unny. 1977. Analysis of heat transfer by natural convection across vertical fluid layers. *Journal of Heat Transfer. Transactions of the ASME* 99:287-293.

Rosenhow, W.M., J.P. Hartnett, and E.N Ganic. 1985. *Handbook of Heat Transfer Fundamentals*, 2d ed. McGraw Hill.

Shewen, E., K.G.T. Hollands, and G.D. Raithby. 1996. Heat transfer by natural convection across a vertical air cavity of large aspect ratio. *Journal of Heat Transfer. Transactions of the ASME* 118:993-995.

Standaert, P. 1984. Thermal evaluation of window frames by the finite difference method. In *Proceedings, Windows in Building Design and Maintenance.* Stockholm: Swedish Council for Building Research.

Wright, J. 1996. A correlation to quantify convective heat transfer between vertical window glazings. *ASHRAE Transactions* 102(1):940-946.

Yuan, S., G. A. Russell, and W. P.Goss. 2002. Uncertainty analysis of a calibrated hot box. In *ASTM STP 1426, Insulation Materials: Testing and Applications*, Vol. 4 (A. P. Desjarlais and R. R. Zarr, eds.). West Conshohocken, PA: ASTM International.

Zhao, Y. 1998. Investigation of heat transfer performance in fenestration system based on finite element methods. Ph.D. dissertation, Department of Mechanical and

Industrial Engineering, University of Massachusetts, Amherst.